Yamato 82192, 82193, 86032

Anorthositic fragmental breccia

37, 27, 648 g

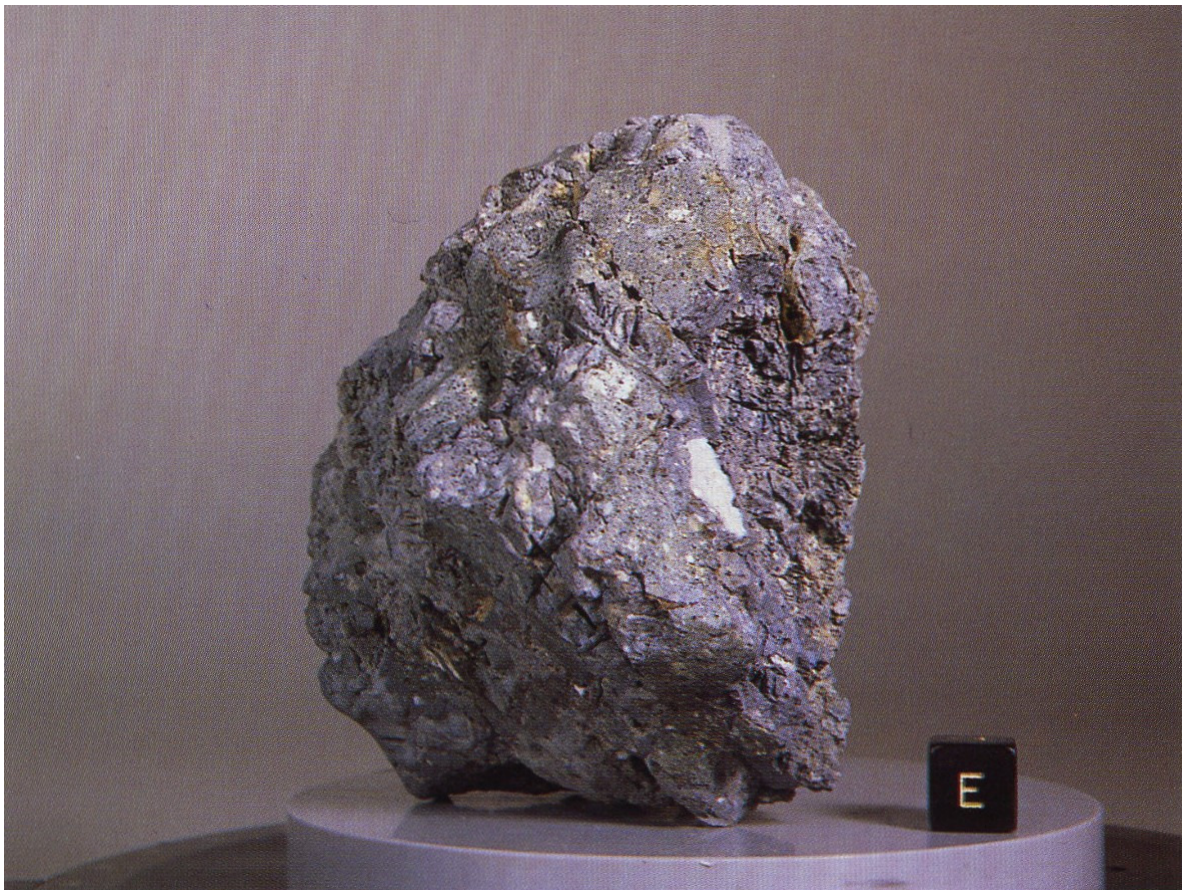

Figure 1: Yamato 86032 in the meteorite laboratory at the NIPR (from Yanai et al., 1987).

Introduction

Yamato 86032 (Fig. 1) was discovered December 9, 1986 during the 27th JARE in the Yamato Mountains (Figs. 2 and 3). It was recognize as similar to Yamato 82192 and 82193, as well as in close proximity. Preliminary examination (Yanai et al., 1987) showed it is an anorthositic breccia. In contains numerous white to grey clasts as well as impact melt veins and deep narrow cavities. It was allocated to 25 international investigators as part of a consortium.

Petrography

Modal mineralogy and detailed petrographic descriptions of the Yamato 86/82 reveal their similar clast mineral content (Table 1). All three meteorites contain matrix that is glass rich, with minor amounts of fine grained mineral clasts including olivine, pyroxene and plagioclase. Clasts present in these meteorites include subophitic impact melt clasts, feldspathic and mafic impact melt clasts and granulitic breccias. All clasts reported so far are feldspathic with a few exceptions: basaltic clasts in Y-82193 (Takeda et al., 1987), and Y-86032 (Yamaguchi et al., 2004, 2008). Typical textures are illustrated in thin section photomicrographs from the NIPR Photographic Catalog (Fig. 4 to 6; Yanai et al., 1987), sketches and images taken by Bischoff et

al. (1987) for the Yamato 82192 and 82193 paired stones (Figs. 7 and 8), and images of a slab of Yamato 86032 studied by Takeda et al. (1999) (Figs. 9 and 10).

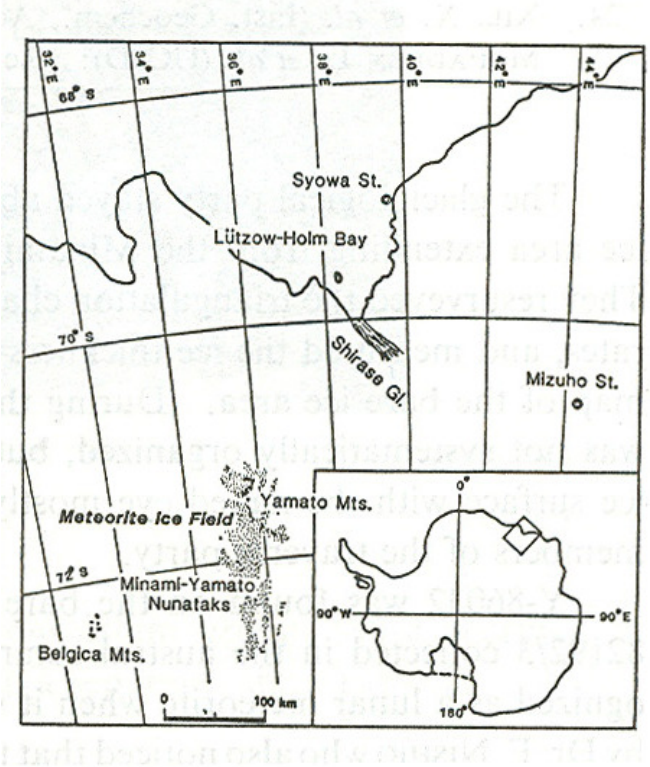

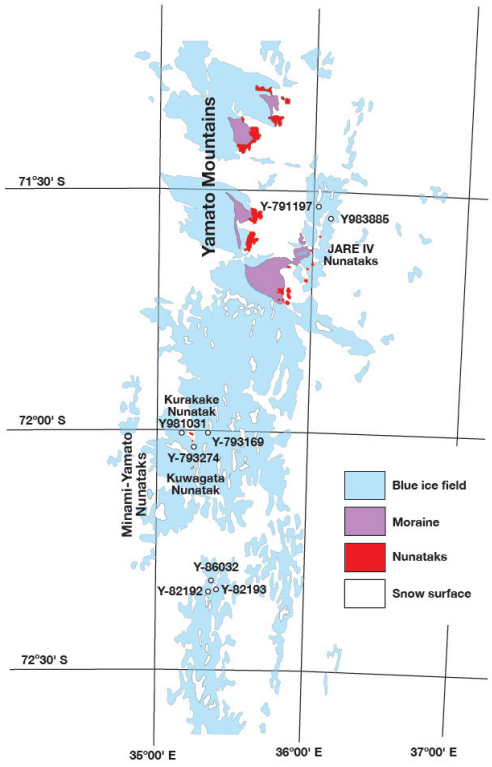

Figure 2: Location map for the Yamato Mountains
Figure 3: Detailed location map for the Yamato lunar meteorites (courtesy of NIPR). The Y86032 and paired meteorites are near the bottom of the map.

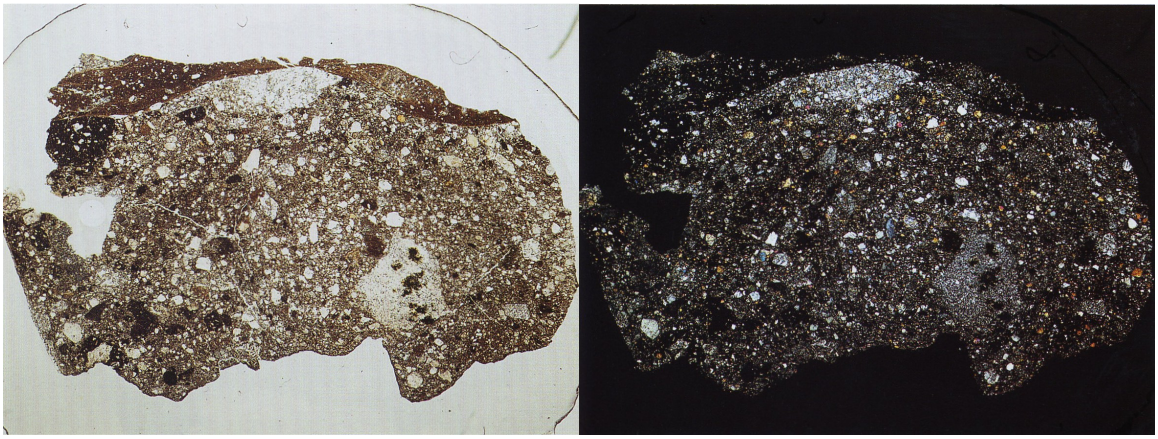

Figure 4: Plane polarized light (top) and crossed polars (bottom) photomicrographs of section 51-1 of Y-86032 (from the NIPR Photographic Catalog; Yanai et al., 1987), illustrating a polymict breccia with feldspar-rich lithic and mineral clasts set into a dark matrix. The largest clast is feldspathic, fine-grained and 5 mm across.

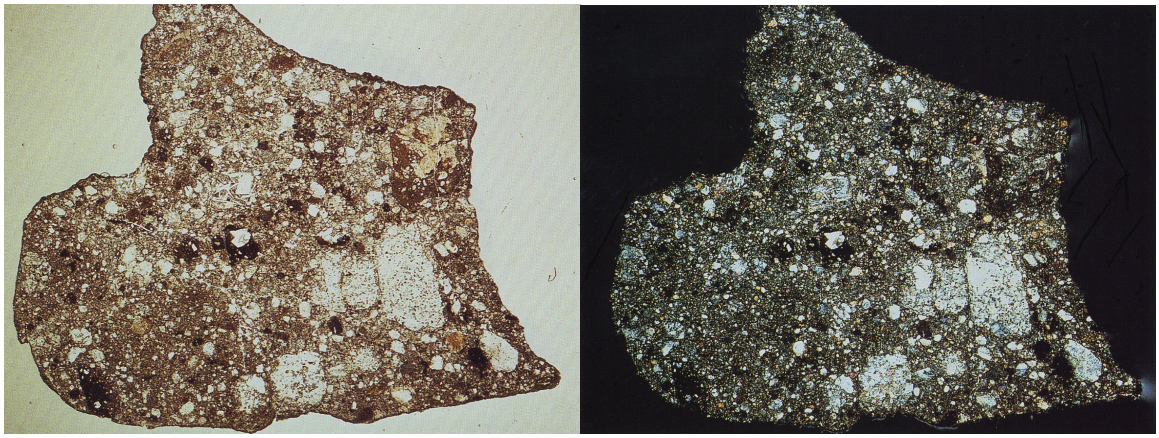

Figure 5: Plane polarized light (top) and crossed polars (bottom) photomicrographs of section 50-3 of Yamato 82192 (from the NIPR Photographic Catalog; Yanai et al., 1987), illustrating a polymict breccia with feldspar-rich lithic clasts (up to 1.5 mm) and mineral clasts set into a light brown matrix. Some clasts are black, with enclosed mineral fragments, and some melt rocks are present. Glass spherules are also observed (long dimension is 11.9 mm).

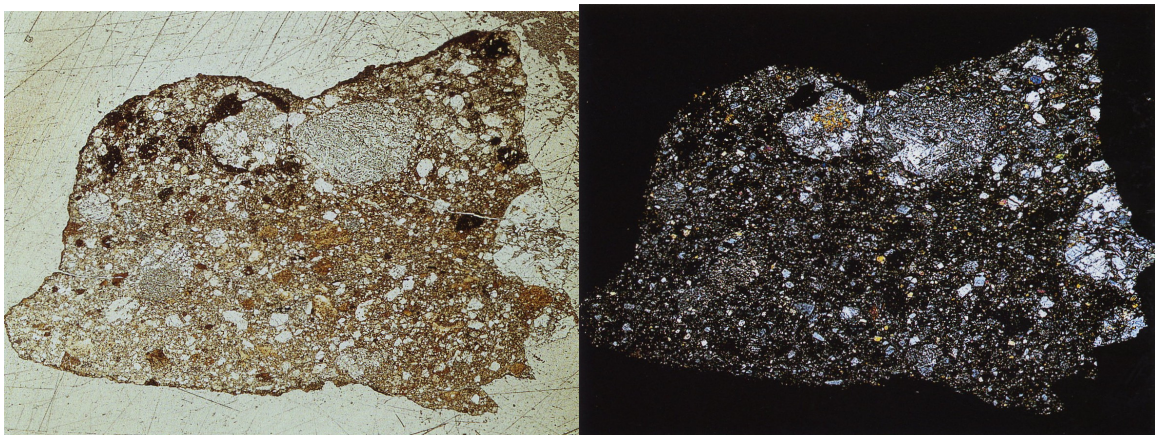

Figure 6: Plane polarized light (top) and crossed polars (bottom) photomicrographs of section 91-1 of Yamato 82193 (from the NIPR Photographic Catalog; Yanai et al., 1987), illustrating a polymict breccia with feldspar-rich clasts (up to 1 mm) and smaller mineral clasts set into a light brown matrix. Glass spherules are also observed (long dimension is 8.2 mm).

Table 1: Clast population of Yamato 82192 and 82193 (Bischoff et al., 1987)

Component	Y-82192	Y-82193
Recrsytallized and granulitic litholgies	49.0	44.4
Feldspathic crystalline melt breccias	14.3	13.0
Mafic crystalline melt breccias	13.2	4.3
Vitric to devitrified (impact) glasses	1.6	40.5
Mineral fragments	10.1	10.5
Feldspathc and mafic basalts	7.8	19.2
Polymict fragmental breccias	2.1	4.0
Others	1.8	-
	99.9	99.9

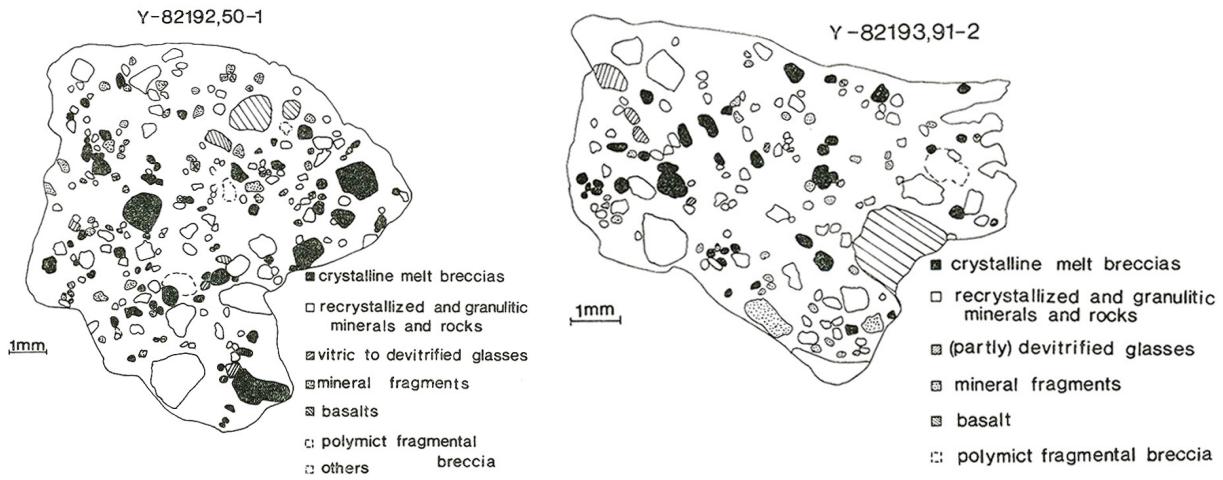

Figure 7: Sketch maps of Yamato 82192 and 82193 showing the distribution of mineral and lithic clasts (from Bischoff et al., 1987).

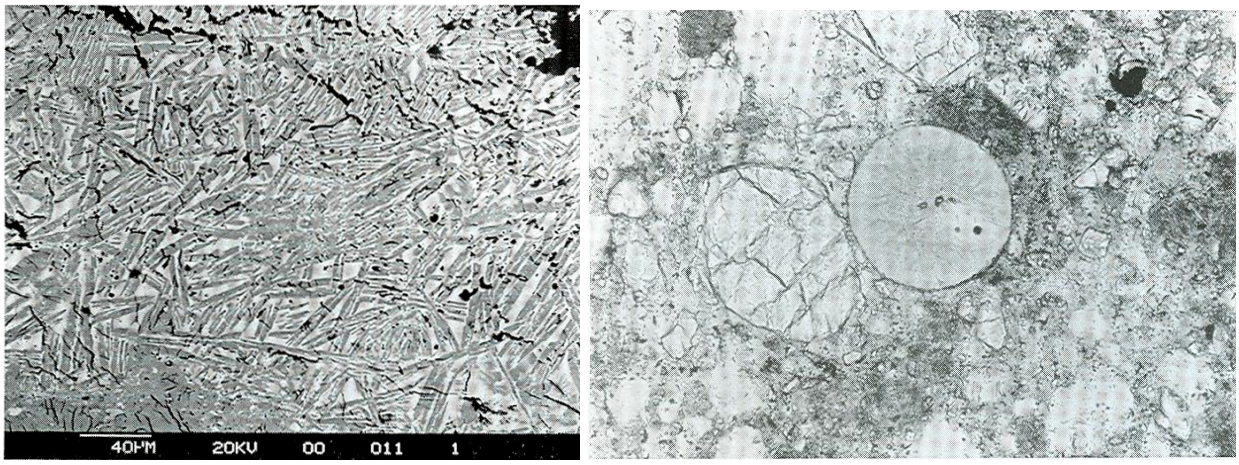

Figure8a: Back scattered electron image of a fine grained impact melt breccia with subophitic to variolitic texture in Yamato 82192 (from Bischoff et al., 1987). Figure 8b: Plane polarized light photomicrograph of a recrystallized spherule embedded in a fine grained matrix in Yamato 82192 (from Bischoff et al., 1987).

Mineralogy

Most mineral fragments and minerals in the clasts define a narrow range compared to many other lunar meteorites. For example, the plagioclase compositions are all very anorthite-rich. The olivine compositions range between Fa_{20} and Fa_{40}. And the pyroxenes are relatively magnesian compared to some of the ferro-augites and ferro-pigeonites reported in other highlands breccias and mare basalts (Fig. 11). In addition, the Mg# and An of coexisting minerals in the clasts are more typical of ferroan anorthsites, but also include some magnesian varieties that are not within the Mg suite region (Fig. 12). It is important to note that the total range of mineral compositions is quite high, from $Fa_{16\text{-}93}$ olivine, and Mg# 0.38 to 0.81 pyroxene (Yamaguchi et al., 2004).

The variety of lithic clasts in the Y-86032 breccia not represented by the Apollo samples indicates that this meteorite was not derived from the central nearside (Nyquist et al., 2006; Yamaguchi et al., 2008). The low bulk FeO and Th abundances suggest that Y-86032 is from a

locality distant from the PKT (Jolliff et al., 2000). Yamaguchi et al. (2008) suggest that Y-86032 was lithified in the highlands between the nearside and farside, and before the Imbrium impact. The basaltic and gabbroic clasts described by Yamaguchi et al. (2004, 2008) in Y-86032 probably originated from such regions, and represent ancient volcanism at prior to 3.8 Ga ago, and before the Imbrium impact.

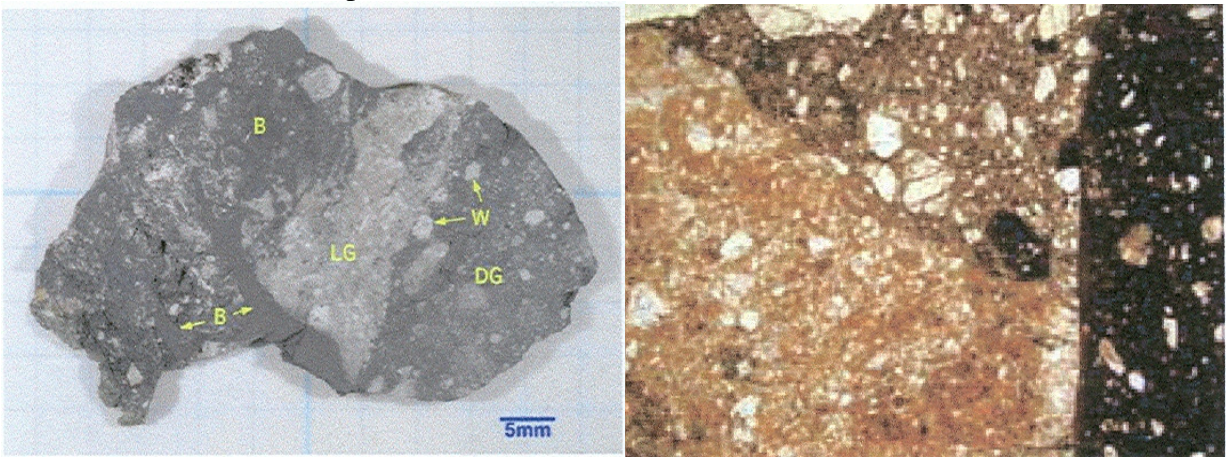

Figure 9: Image of large slab of Y-86032, illustrating the light grey (LG), dark grey (DG), white clast (W) and black shock (B) lithologies (from Yamaguchi et al., 2004).

Figure 10: Close up image of a grey clast region of Y-86032 (from Takeda et al., 2002). This is not the same grey clast lithology as in Figure 9.

Chemistry

Major element compositional characteristics of the Yamato 86/82 meteorites are similar to other feldspathic regolith breccias having between 25 and 30 wt% Al_2O_3, and Mg# from 62 to 69, and Fe/Mn ratios between 68-76 (Table 2a and 2b). These meteorites all have Eu anomalies, but have very low rare earth element and other incompatible element concentrations (Figs. 13 and 14). With REE contents this low, it is clear that no KREEP component is present. It should be noted, however, that despite the low concentrations of incompatible elements, the Y-82/86 meteorites contain the highest Na, Sr, and Eu contents of any of the lunar feldspathic meteorites, which is a reflection of their higher plagioclase Ab content (Korotev et al., 2003; Yamaguchi et al., 2004).

Detailed work on C and N was reported by Grady and Pillinger (1990). There are two high temperature components, one released at 550 to 700 °C, and the other at 900 to 1100 °C. These two components have not been observed in other pristine lunar breccias, and could be from a component inherited from Antarctica (but unlike any carbonate reported previously), from an unsampled lunar environment, or perhaps most likely from material provided by the impactor (Grady and Pillinger, 1990). Finally, the very low noble gas concentrations (Fig. 15) indicate only a brief exposure to solar wind at the surface of the Moon, suggesting that these meteorites represent pieces of an immature regolith.

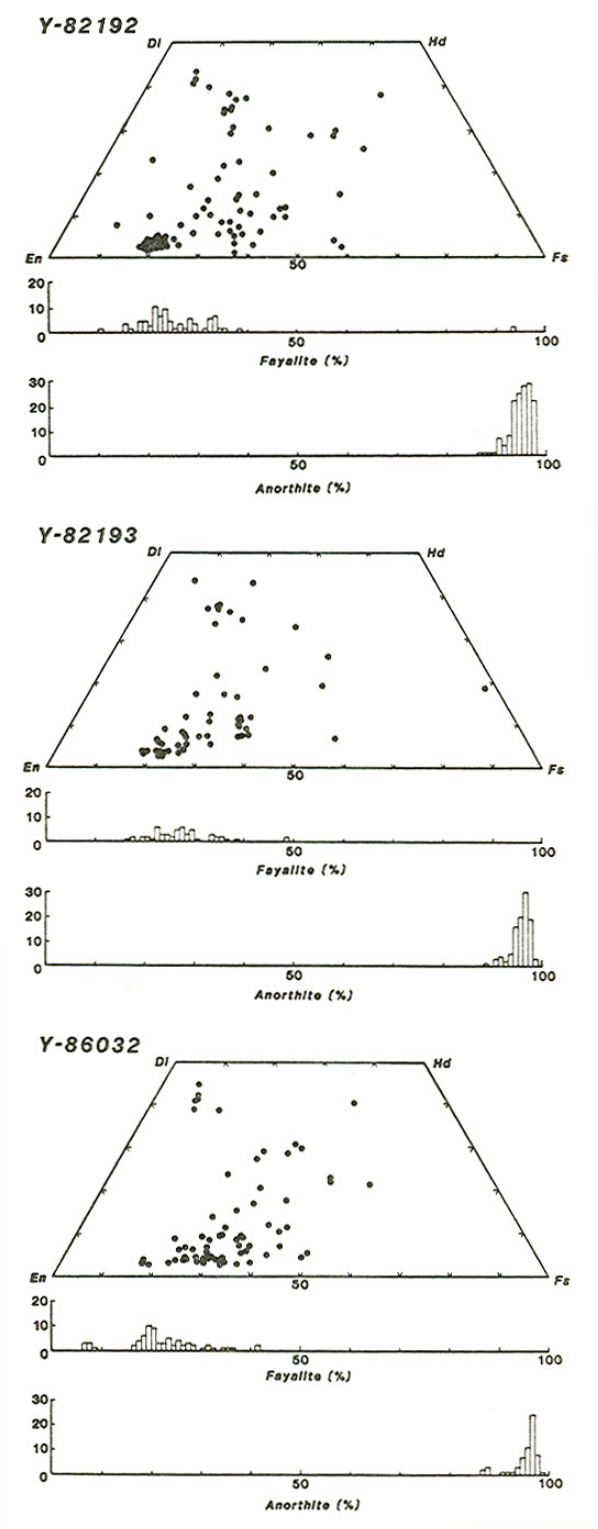

← *Figure 11: Pyroxene quadrilateral diagrams, and olivine and plagioclase histograms for Yamato 86032, 82192 and 82193 (from Yanai and Kojima, 1991).*

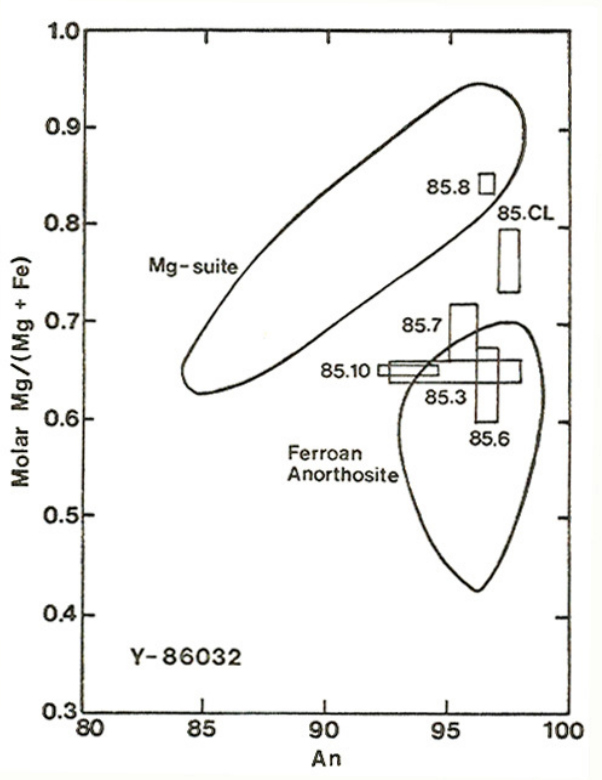

Figure 12: An vs. Mg# for clasts from Y-86032 illustrating the overlap with FAN suite rocks, and the intermediate samples (from Koeberl et al., 1990).

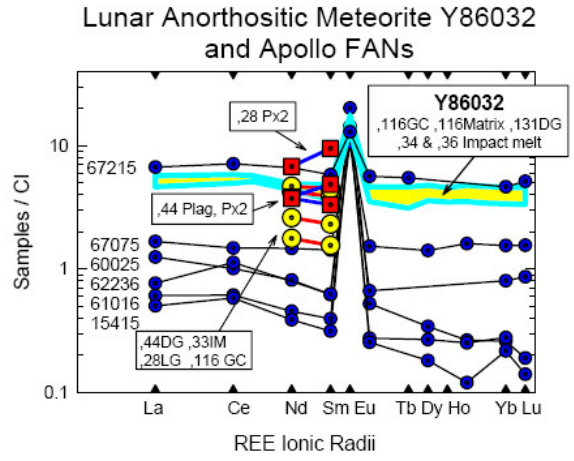

Figure 13: REE determinations for the Yamato and MAC lunar meteorites compared to norites and FAN's (from Nyquist et al., 1999, 2005).

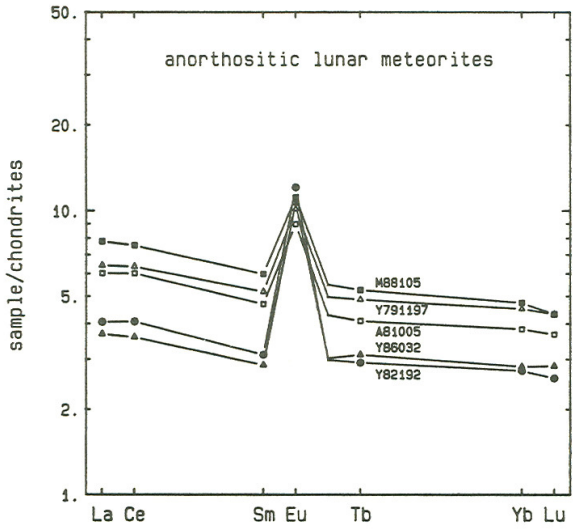

Figure 14: REE determination for Yamato and other anorthositic lunar meteorites (from Lindstrom et al., 1991).

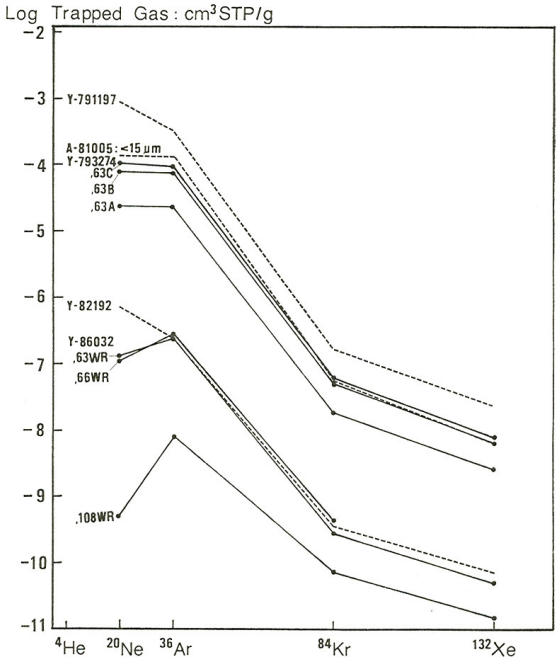

Figure 15: Noble gas concentrations for the Yamato lunar meteorites from Takaoka and Yosida (1997).

Table 2a: Chemical composition of Yamato 86032

reference	1	2	3	1	1	4	1	1	8	8	8	9	9
									34, B	36, B	131,	Mean 1	Mean 2
split	,84	,78	,75/6		,64	,86					DG		
Wt. (mg)	70	244	229.3	122									
method	e	e	e	e	e	e	e	e	b,c,e	b,c,e	b,c,e		
SiO_2 %	0.00	45.11	42.98	0.00	0.00	0.00	43.64	44.09	45.54	44.47	44.05	44.9	44.6
TiO_2	0.00	0.25	0.19	0.20	0.20	0.10	0.03	0.20	0.12	0.18	0.23	0.181	0.20
Al_2O_3	0.00	27.77	29.37	27.58	28.14	0.00	29.07	29.24	28.71	28.52	30.22	29.6	28.5
FeO	4.12	4.22	4.19	4.36	4.28	3.73	5.03	4.21	4.41	4.45	5.00	4.06	4.28
MnO	0.05	0.06	0.06	0.06	0.06	0.00	0.03	0.06	0.05	0.05	0.06	0.0624	0.0607
MgO	0.00	5.56	5.07	5.94	4.81	0.00	5.03	5.24	6.29	5.57	5.54	5.10	5.36
CaO	0.00	15.67	16.65	16.09	16.23	0.00	16.62	16.23	15.39	15.39	15.81	16.4	16.0
Na_2O	0.43	0.45	0.42	0.40	0.42	0.39	0.44	0.43	0.46	0.53	0.50	0.557	0.45
K_2O	0.02	0.03	<0.048	0.02	0.01	0.02	<0.019	0.02	0.00	0.00	0.00	0.039	0.020
P_2O_5	0.00	0.00	0.03	0.00	0.00	0.00	0.06	0.03	0.00	0.00	0.00		
S %													
sum												101.0	99.6
Sc ppm	7.26	8.1	8.46	8.84	8.69	7.3		8.27	8.56	10.32	10.34	8.34	8.30
V		30		28	25			29	35.1	18.5	38.8	27.2	26.0
Cr	660	660	693	724	527	710		666	648	605	752	563	674
Co	13.2	14.4	14.4	14.8	14.9	13.1		14.4	16.2	14.0	16.3	13.3	14.7
Ni	150	115	132	130	155			131	130	110	115	97.1	130
Cu													
Zn	10	6.4		14				9.1					
Ga	4.8	3.4		3.54				3.66	3.65	2.86	-		
Ge													
As	0.27			<0.01				0.27					
Se	0.3		0.44	<0.5				0.4					
Rb	<10			<1				<1					
Sr	118	160	169	174				161					
Y						4.6		4.6					
Zr	25	29		23		17		27					
Nb													
Mo													
Ru													
Rh													
Pd ppb													
Ag ppb				<80				<80					
Cd ppb													

In ppb												
Sn ppb												
Sb ppb	<50			<15			<15					
Te ppb												
Cs ppm	0.05	<0.14	0.046	<0.05			0.05					
Ba	30	26	30	23	24		27	41.0	48.2	44.8	39.6	24.4
La	1	1.56	1.25	1.35	1.25	1.1	1.33	1.28	1.34	1.30	1.20	1.30
Ce	2.6	4	3.42	3.36	3.3		3.51	3.15	3.26	3.25	2.93	3.37
Pr								0.456	0.509	0.464	0.428	0.45
Nd	1.73	2	1.9	1.7	1.9		1.88	1.99	2.21	2.00	1.86	2.01
Sm	0.57	0.66	0.62	0.655	0.61	0.63	0.63	0.586	0.708	0.584	0.561	0.602
Eu	0.87	1.03	0.926	0.858	0.8	1	0.93	0.894	0.988	0.928	1.01	0.928
Gd	1.1						1.1	0.692	0.915	0.702	0.681	0.847
Tb	0.21	0.144	0.132	0.145			0.147	0.129	0.168	0.129	0.125	0.132
Dy	1.1	1.21		0.99	0.7		1.05	0.87	1.16	0.873	0.843	0.996
Ho				0.23			0.23	0.194	0.253	0.194	0.186	0.210
Er								0.559	0.760	0.570	0.544	0.61
Tm				0.12			0.12	0.0827	0.113	0.0847	0.0805	0.112
Yb	0.595	0.61	0.562	0.647	0.59		0.6	0.547	0.747	0.589	0.543	0.583
Lu	0.089	0.086	0.084	0.094	0.089		0.087	0.0813	0.111	0.0844	0.0795	0.0842
Hf	0.54	0.47	0.46	0.47	0.39	0.24	0.47	0.454	0.408	0.400	0.402	0.426
Ta	0.07	0.061	0.057	0.055		0.1	0.06					
W ppb	0.3			<0.08		0.47	0.36					
Re ppb												
Os ppb												
Ir ppb	8.5	5.7	3.9	5.9	4.3		5.3				6.5	5.3
Pt ppb												
Au ppb	6	1.8	3	1.3	1.4		2.4					
Th ppm	0.22	0.25	0.22	0.21	0.2		0.22	0.185	0.171	0.191	0.156	0.198
U ppm	0.07	0.062	0.043	0.05	0.032		0.051	0.0530	0.0518	0.0564	0.0468	0.0534

technique (a) ICP-AES, (b) ICP-MS, (c) PGA, (d) FB-EMPA, (e) INAA, (f) RNAA, (g) XRF

Table 2b: Chemical composition of Yamato 82192 and 82193

	82192	82192	82192	82192	82193	82913
reference	5	2	6	9	7	9
split				mean		Mean
Wt. (mg)						
method	e	e	e		e	
SiO_2 %	0.00	0.00	0.00	45.8	0.00	44.5
TiO_2	0.00	0.35	0.42	0.32	0.27	0.23
Al_2O_3	0.00	25.31	25.56	26.3	25.78	26.7
FeO	6.24	5.75	6.10	5.47	5.63	4.97
MnO	0.10	0.08	0.08	0.0821	0.08	0.0704
MgO	0.00	5.31	5.75	5.41	5.11	5.55
CaO	0.00	14.27	14.83	12.71	16.65	16.23
Na_2O	0.39	0.37	0.36	0.402	0.40	0.416
K_2O	0.02	0.02	0.02	0.040	0.04	0.029
P_2O_5	0.00	0.00	0.00		0.00	
S %						
sum				96.6		98.9
Sc ppm	13.8	13.5	14.5	12.02	12.2	9.95
V		36	41	36.35	31	31
Cr	1156	1010	1020	944	1053	870
Co	18.6	16.7	19.9	16.9	19.2	17.6
Ni	159	122	120	129	148	145
Cu						
Zn		7.3	30			
Ga	10.4	2.8	3.78			
Ge						
As	0.028		<0.2			
Se	0.3		<0.2			
Rb	3		<3			
Sr	150	143	136		180	
Y						
Zr	30	24				
Nb						
Mo						
Ru						
Rh						
Pd ppb						
Ag ppb						
Cd ppb						

In ppb						
Sn ppb						
Sb ppb	<100		<100			
Te ppb						
Cs ppm	0.08	<0.16	<0.1			
Ba	20	22	21	23.0	28	28.0
La	1.11	1.54	1.13	1.16	1.27	1.30
Ce	2.77	3.78	2.98	2.94	3	3.45
Pr				0.32		
Nd	2.1	2.32	1.97	1.86	2	2.00
Sm	0.627	0.68	0.631	0.583	0.65	0.620
Eu	0.779	0.87	0.754	0.830	0.82	0.875
Gd	1			0.707	0.57	0.570
Tb	0.21	0.174	0.17	0.147	0.14	0.145
Dy	1.08	1.28	1.13	1.012	1	0.865
Ho		0.243	0.26	0.221		0.170
Er				0.510		
Tm	0.1			0.091		
Yb	0.71	0.79	0.76	0.632	0.73	0.645
Lu	0.1	0.121	0.115	0.0963	0.117	0.0985
Hf	0.92	0.73	0.44	0.501	0.45	0.435
Ta	<0.1	0.038			0.034	
W ppb						
Re ppb						
Os ppb						
Ir ppb	10	6.4	5.6	5.3	5.7	5.9
Pt ppb						
Au ppb	3.1	1.4	1.1		1.3	
Th ppm	0.23	0.188	0.2	0.160	0.2	0.195
U ppm	0.066	0.058	0.05	0.0478	0.04	00485

technique (a) ICP-AES, (b) ICP-MS, (c) PGA, (d) FB-EMPA, (e) INAA, (f) RNAA, (g) XRF

Table 2c. Light and/or volatile elements for Y86032, Y82192, and Y82193

	86032	86032	86032	86032	86032	86032	86032	86032	82192	82192	82192	82193
reference	1	2	3	1	1	4	1	1	5	2	6	7
split	,84	,78	,75/6		,64	,86						
weight	70	244	229.3	122								
Li ppm												
Be												
C												
S												
F ppm												
Cl	<30			<50				<30				
Br	<0.2	0.12		<0.1				0.12	0.08	<0.17	<0.2	
I												
Pb ppm												
Hg ppb	<0.07			<0.1				<0.07	<0.05			
Tl												
Bi												

References for Tables 2a,b,c: 1) Koeberl et al. (1989); 2) Warren and Kallemeyn (1987); 3) Lindstrom et al. (1991); 4) Eugster et al. (1989); 5) Koeberl (1988); 6) Bischoff et al. (1987); 7) Fukuoka et al. (1986); 8) Karouji et al. (2004); 9) Nyquist et al. (2006).

Radiogenic age dating

A very old plateau age of 4.4 Ga was obtained on a feldspathic clast from Y-86032 by Bogard et al. (1999) (Fig. 16). This ancient age is supported by a similarly old model age determined by Nyquist et al. (1999, 2005) (Fig. 17). Furthermore, an affinity to ancient FAN lithologies, such as 60025, has been known since the Pb isotope measurements of Tatsumoto and Premo (1991) on Y-86032 and Y-82192 (Fig. 18).

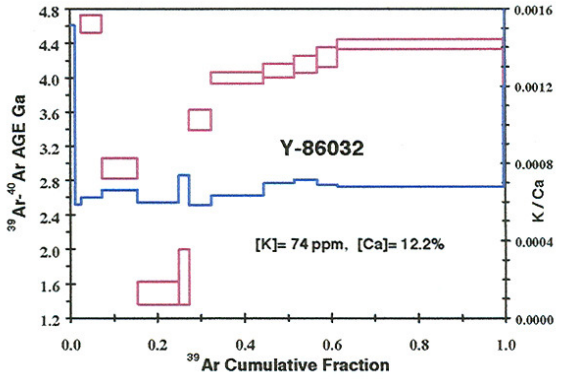

Figure 16: Ar-Ar plateau age of 4.4 Ga for a clast from Y-86032 (from Bogard et al., 1999).

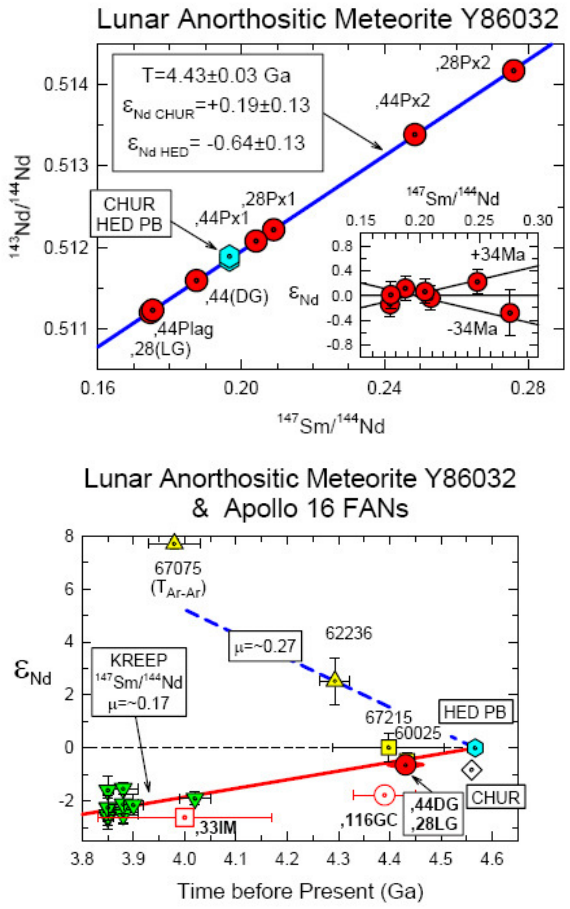

Figure 17a: Sm-Nd isochron for Yamato 86032 (from Nyquist et al., 1999, 2005); Figure 17b: Nd model age for Yamato 86032 (from Nyquist et al., 1999, 2005).

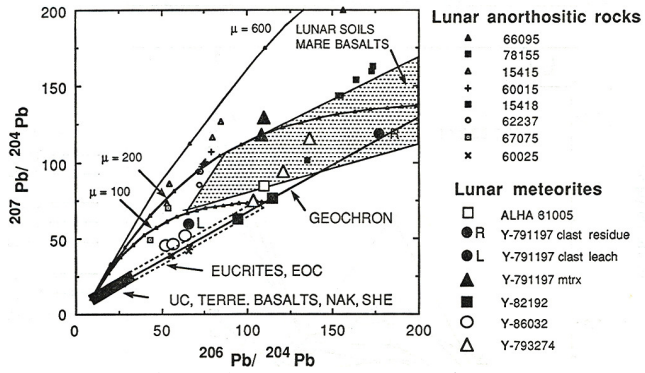

Figure 18: Pb isochron for Yamato 86032 (open circles) from Tatsumoto and Premo (1991).

Cosmogenic isotopes and exposure ages

Noble gas studies of Y-82192, Y-82193, and Y-86032 have all yielded similar terrestrial ages of 72,000 +/- 30,000 yrs (Eugster et al., 1988, 1989). Similarly cosmic ray exposure ages are all near 11 Ma (4 pi exposure age) (Eugster, 1988). Also gleaned from this work are K-Ar ages for Y-86032 that are 3680 +/- 300 Ma and 3810 +/- 400 Ma (Eugster et al., 1989), also consistent with the old age of clasts determined in studies cited above.

Processing

Dozens of sample splits of Y-86032 were generated and allocated in 1987 to 1988 to researchers all around the world. These are summarized in Table 3, compiled from information published by Takeda et al. (1989). Pre-processing photographs were taken of all three meteorites and published in the NIPR Photographic Catalog (Yanai and Kojima, 1987) (Figures 19 - 21).

Table 3: Processing history of Yamato 86032 (from Takeda et al., 1989).

Split	Parent	PTS	Wt.	Location	description
20			6.898	subdivided	
21				NIPR	Figure 9; slab
51		X	2.136	NIPR	Thin section butt
52	20		3.273		
53	20		3.033		
54	53		1.033	Nagao	geochemistry

55	53		0.215	Nishiizumi	Exterior, exposure ages
56			0.788	Kushiro	Bulk chemistry
61			1.063	subdivided	
62			0.110	subdivided	
63			0.224	Takaoka	Matrix, noble gases
64	62		0.100		Clast and matrix, INAA
65	62	X	0.010		Clast
70			0.163	Pillinger	Interior, stable isotopes
71	62		1.191	subdivided	US splits
81			0.170		fragments
82	20		0.336	subdivided	clast
83	20	X	0.182	NIPR	Thin section
84			0.309	Koeberl	Impact melt, halogens
85			0.315	Koeberl	Bulk, halogens trace elements
86			0.420	Eugster	Bulk, Noble gases
87			0.376	Nagata	Magnetic study
88			0.113	Wänke	Trace elements
89			0.143	Stöffler	Petrography, shock
90			0.028	Stöffler	Petrography, shock
91	20		0.074		
92	82		0.143	Kaneoka	Clast, noble gases
93	61		0.022	Warren	INAA
95	61		0.175	Masuda	Clast, REE
97	61	X	0.008		Clast
98	61		0.310	Masuda	Matrix, REE
99	61		0.048	Kaneoka	Matrix, noble gases
106	61		0.008	Fukuoka	Clast, INAA
107	61	X	0.003	Fukuoka	clast
108	82		0.071	Takaoka	Clast, noble gases
109			0.013	Fukuoka	Glass, INAA

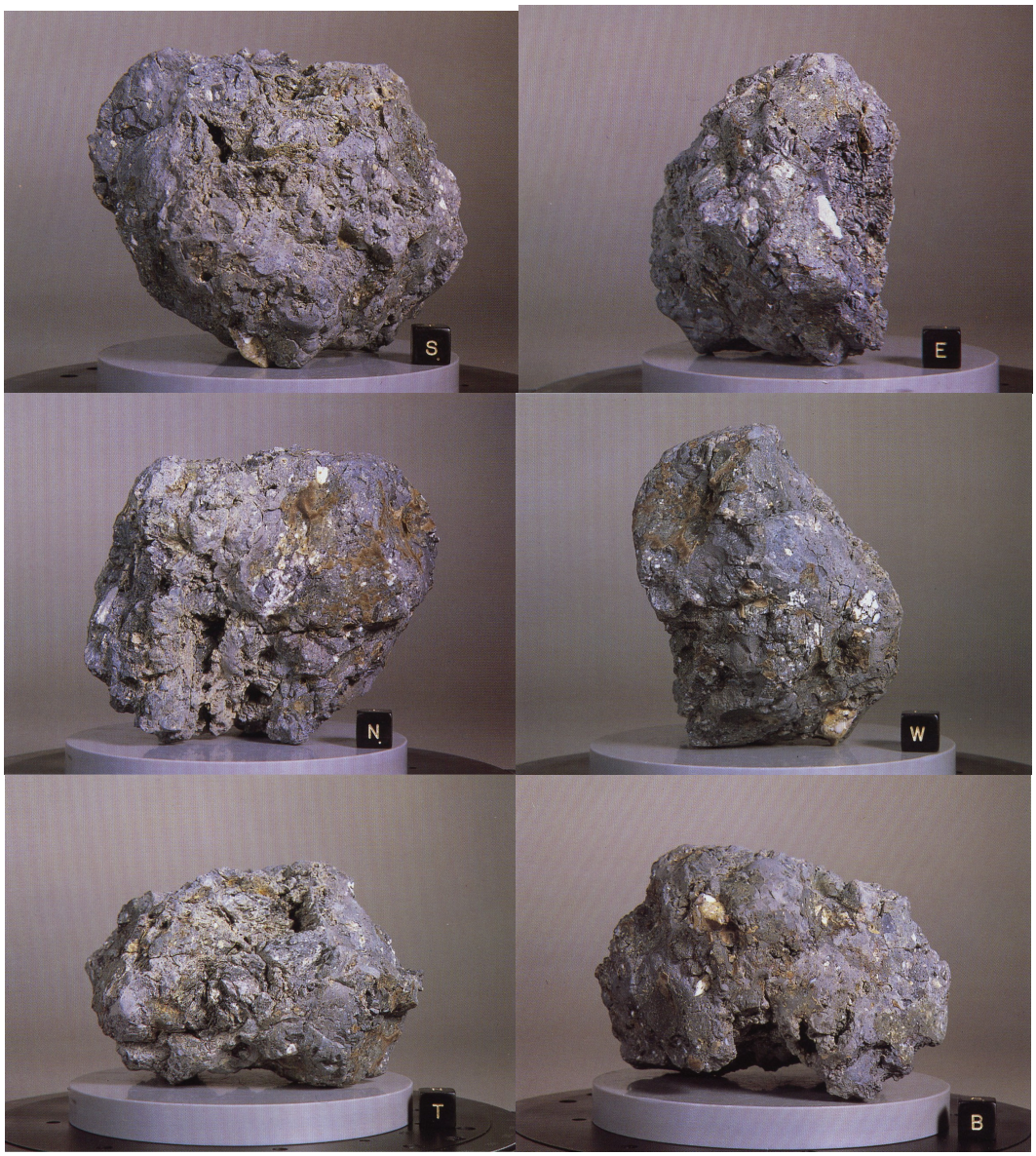

Figure 19: Six views of Y-86032, from Yanai and Kojima (1987).

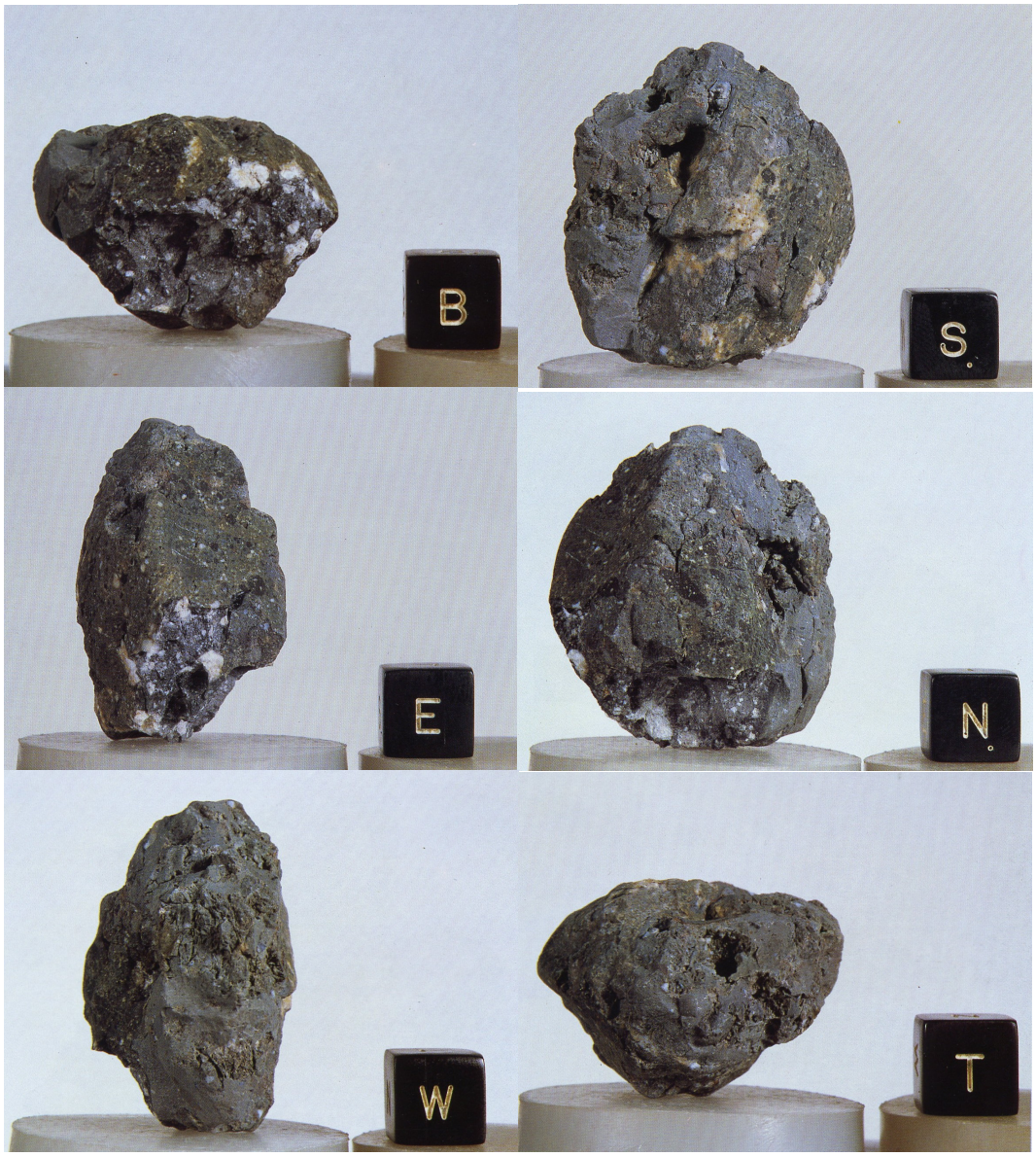

Figure 20: Six views of Y-82192, from Yanai and Kojima (1987).

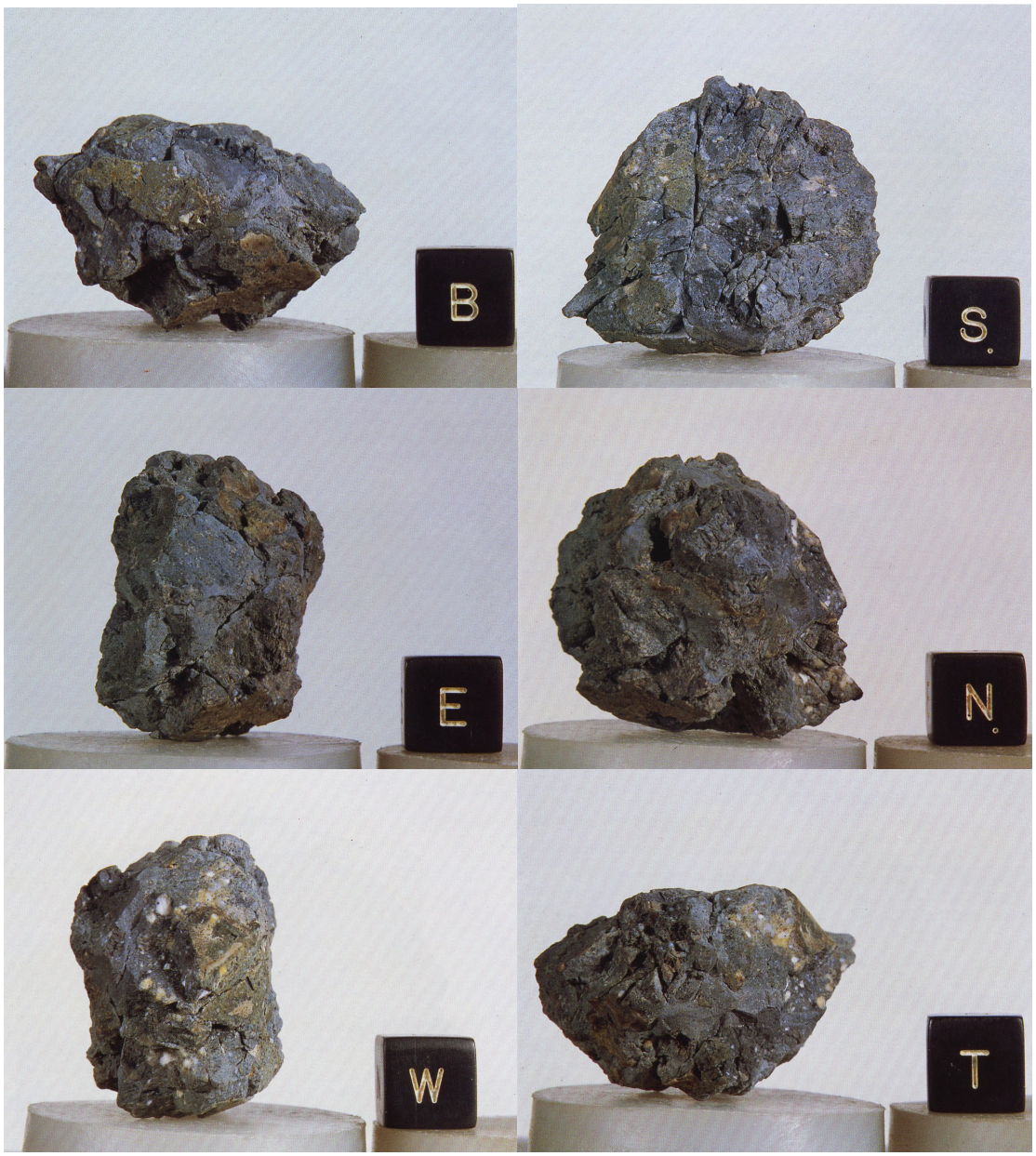

Figure 21: Six views of Y-82193, from Yanai and Kojima (1987).

Lunar Meteorite Compendium by K Righter 2010